Journal of the British Interplanetary Society, Volume 68, 2015, pp. 188-199
Refcode: 2015.68.188, https://www.jbis.org.uk/year/2015

INVESTIGATIONS OF A COMBUSTIBLE INERTIAL LAUNCH VEHICLE DESIGN

VITALY YEMETS[1], SIMON PRINCE[2] AND RAY WILKINSON[3]
1. *Physical-Technical Faculty, Dnipropetrovs'k National University, 72 Gagarin Avenue, 49010 Dnipropetrovs'k, Ukraine.*
2. *School of Engineering and Mathematical Sciences, Centre for Aeronautics, City University London, Northampton Square, EC1V OHB, London, UK.*
3. *School of Engineering and Technology, the University of Hertfordshire, College Lane, Hatfield, Hertfordshire, AL10 9AB, UK.*
Email: vitaly.yemets@yahoo.com[1], s.a.prince@city.ac.uk[2], r.wilkinson@herts.ac.uk[3]

The paper develops a subject of a combustible inertial (self-feeding) launch vehicle for nano and pico satellites. A part of the paper considers a flight of the rocket using ballistic, aerodynamic and thermal calculations. Another part describes experimental investigations of a laboratory-scale model of the rocket engine. Plans for future work and prospects of the self-feeding technology combined with pulse engine mode for microlaunchers and small satellite micro propulsion concludes the paper.

Keywords: Combustible inertial LV, self-feeding rocket propulsion

1. INTRODUCTION

The engineering feasibility of an extremely small launch vehicle (LV) intended to put into an orbit nano- and picosatellites and suitable to be served by a small scientific team was considered in [1] several years ago. It was called as combustible inertial LV (CILV) and based on the following non-traditional principles: (1) burning the rocket structure as main propellant, (2) the gasification of the structure before feeding it into the rocket engine and (3) the use of inertial forces to deliver propellant into the engine – so no feed device. According to [1] these three items would make a CILV really small, light and suitable for handling: about 6 m in length, 0.2 m in diameter and 300 kg of initial mass if payload was 1 kg (about 0.3 percent of the initial mass). Moreover the important advantage of the CILV is its unusual staging structure. Its first stage relative final mass was designed to be equal to 0.05 (in contrast to traditional 0.2...0.3) to get the final equivalent speed of about 6 km/s to ensure that the first stage burns down in the atmosphere after the stage separation. Such a design was called a quasi single-stage design because like a real single-stage LV it did not need impact areas for jettisoned parts.

As a payment for the extremely simple structure an unusually high g-load characterized the rocket, which resulted from the necessity to get an acceptable pressure of the inertial feed of gasiform propellant into the engine. Accelleration was 10 g at the initial phase of the first stage flight and about 70 g at its final phase. Although according to [1] the maximum theoretical feeding pressure could be about 2 MPa, the vehicle design is limited by practical issues such as rocket length and an acceptable initial g-load. Combustion pressure varied from 0.8 MPa at the start to 0.4 MPa at the end of the first stage for the 6-metres-in-length vehicle. The CILV structure was designed with the intention to limit g-loading at the final phase of the first stage flight. The stage therefore consisted of two parts: one part was propelled with full initial thrust and another one was driven with a fraction of the trust. In short, small dimensions and mass, quasi single-stage structure, high g-loading and low engine pressure were the main distinguishing features of the launcher. While the third and forth features could be considered as disadvantages, the first and second ones made the design quite attractive for further development.

Since the mass and dynamic characteristics of the CILV were estimated in [1] with rough calculations, the detailed investigation of the rocket flight taking into consideration its trajectory, aerodynamic and thermal loads are necessary to verify the estimation. This is the first subject of the investigation presented in this paper.

The important design assumptions made in [1] were lightness and simplicity of the CILV engine, which is designed to be made of thin conical steel shells and powered with a propellant charge consisting of coaxial layers of fuel and oxidizer. However, such a propellant charge was not tested previously with such an engine. The second subject of this work is therefore an experimental verification of the engine engineering feasibility.

2. INVESTIGATING CHARACTERISTIC FEATURES OF THE ROCKET LAUNCH

The theoretical investigation of the CILV flight was undertaken at the Centre for Aeronautics, City University London. There were three phases of the investigation: (1) the calculation of the rocket trajectory in a first approximation – launching the rocket of the initial design presented in [1], (2) the evaluation of the thermal and pressure loads experienced on the rocket air frame during ascent and (3) the correction of the LV design and trajectory to decrease the loads under an acceptable level.

Copyright © The Authors. Published by JBIS. This is the Author Accepted Manuscript issued with: Creative Commons Attribution Non-Commercial License CC:BY:NC 4.0).

In the first phase a launch trajectory was calculated with the FNA prediction programme developed at Moscow Aviation Institute in 1980s and published in [2]. The launch vehicle presented in [1] was considered as a point mass. At the very beginning an attempt to apply a conventional flight programme was made: after a vertical launching the rocket pitch angle fell from 90 deg to 20-30 deg as a parabolic function of time and after the first stage separation the pitch angle linearly diminished to 0. The attempt was unsuccessful because the high atmospheric losses of speed resulted in a negative value of payload. To decrease the atmospheric losses, the terminal pitch angle of the first stage was increased and a pause between the first stage separation and the second stage activating (at an altitude of about 100 km) was inserted. In order to meet the criterion for maximum payload in a circular orbit with an altitude of 300 km, analysis showed that the 1st stage terminal pitch angle should be 45 degrees with a 30 second pause before 2nd stage ignition.

Nevertheless, it was found that aerodynamic drag forces during the initial launch phase was too high, resulting in a 2.8 km/s decrease in desired speed at first stage burnout, which decreased the payload to about 0.2 percent of the initial mass instead of 0.3 percent expected in [1]. The high g-loading during 1st stage flight, resulting in excessive speeds at low altitudes where atmospheric density is greatest, as shown in Fig. 1, clearly needed revision.

In addition to the drag forces, the thermal loads were also investigated using an axisymmetric Navier-Stokes solver, which was used to calculate flow solutions assuming perfect gas behaviour for freestream Mach numbers up to 4.0, and employing a real gas model for equilibrium gas chemistry involving six chemical species (O_2, N_2, O, NO, N and Ar) in three reactions for Mach numbers between 4.0 and 6.0. Each calculation, for a given point in the trajectory, was computed on its own computational structured grid, according to the vehicle geometry at that stage of the launch, which consisted of between 50,000 cells (full length vehicle at Mach 0.1) to 28,000 cells for the configuration at the beginning of first stage restricted thrust flight (see Fig. 5). All flows were assumed to be steady and axisymmetric (zero angle of attack). The CILV layout and dimensions presented in [1] were used for these calculations, and conical fairings covering the rocket nose and interstage flare regions were added, as seen in Fig. 3.

Figure 2 shows that according to these calculations boundary layer surrounded the cylindrical part of the rocket was heated to about 400 K at 5.5 s since its launching, to 730...740 K at 10

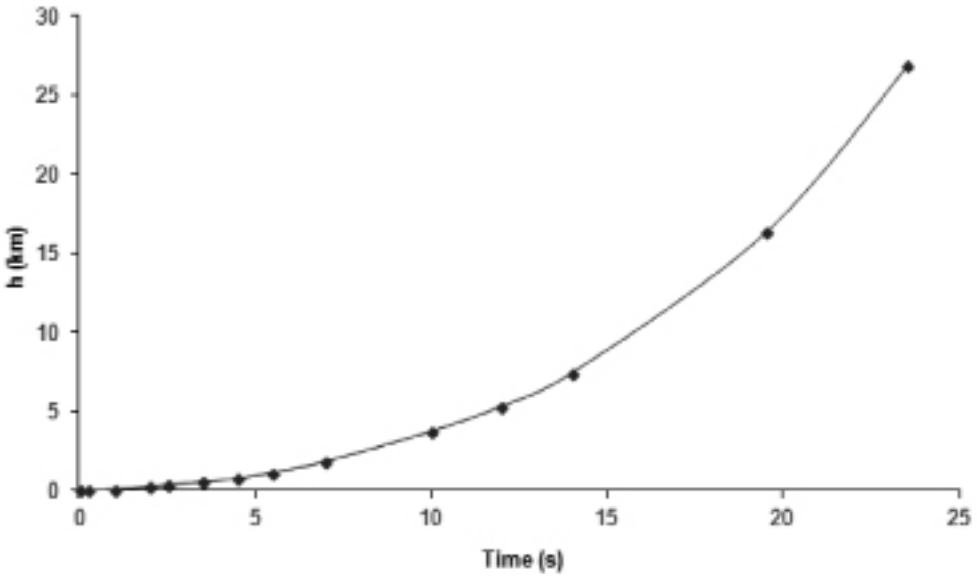


Fig. 1 The flight altitude and Mach vs. flight time for the initial version of the CILV first stage.

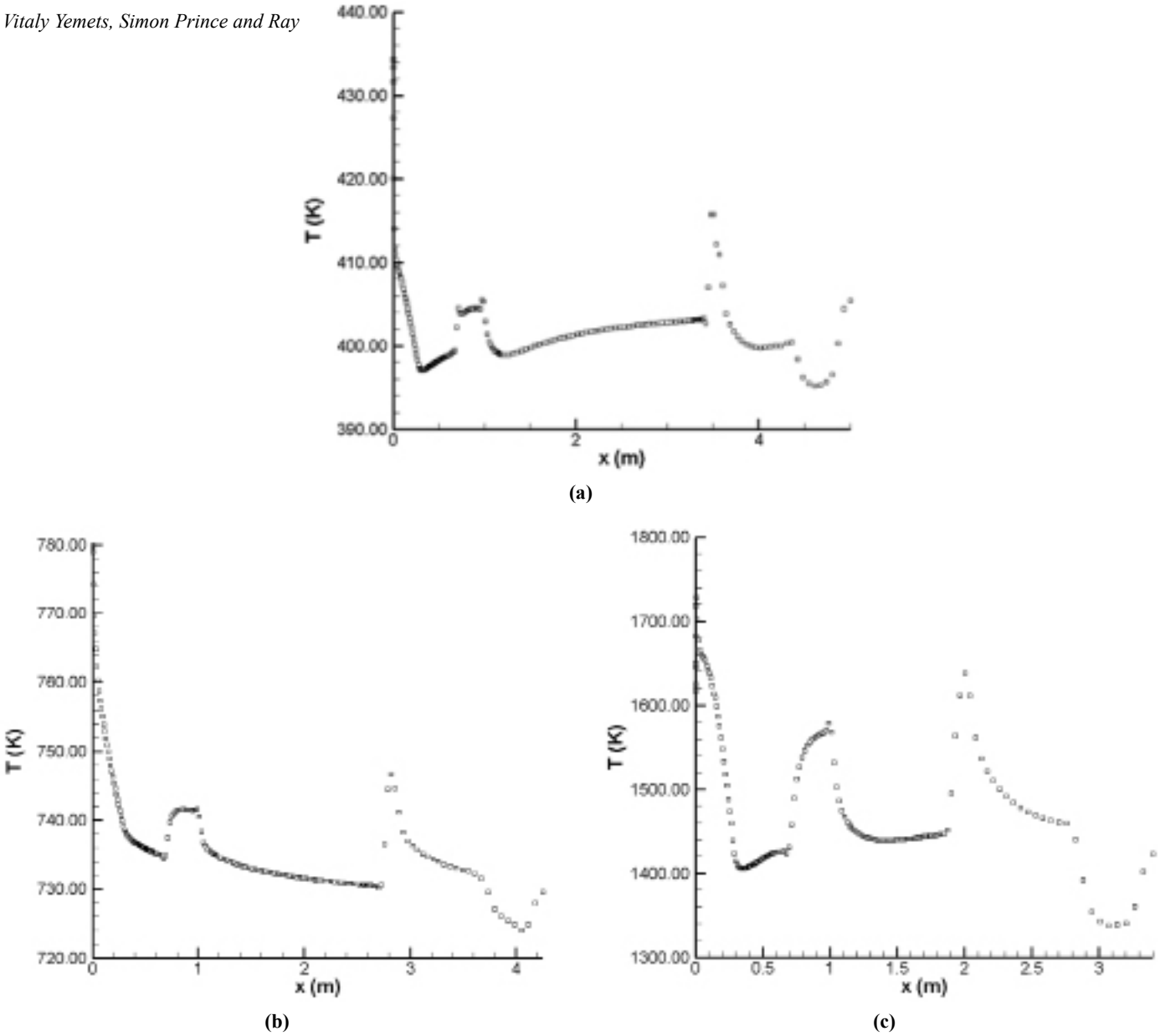


Fig. 2 The temperature of the contracting rocket airframe surface at the following instants of time following the rocket launch: (a) 5.5 s, (b) 10 s, (c) 14 s.

s and to 1400...1430 K at 14 s. The first figure approximately equals the initial melting temperature of polyethylene or maximum operating temperature of polypropylene; the second range is somewhat more than the minimal temperature of polytetrafluoroethylene pyrolysis, and the third range is close to the melting points of steels. It means that if the rocket shell was made of polyethylene or polypropylene an outer layer of the shell could be melted at 5 or 6 second after launch; if the shell was covered with polytetrafluoroethylene the layer could be destroyed at 9 or 10 second, and the steel shell would begin to melt at 14 seconds after launch. So to prevent the rocket structure melting and make the launch trajectory more suitable we need to change the flight programme or/and the rocket layout and structure.

Figure 3 shows the aerodynamic pressure in the flowfield around the launcher under maximum load, which was not considerable, at about 0.15 MPa. It was therefore deemed to be a relatively simple job to design the vehicle airframe to have sufficient structural strength.

At the third phase of the investigation the input data and the rocket layout were corrected and another launching trajectory was calculated taking into account the maximum acceptable specific heat flow q_{max} directed to the rocket. As it is known the specific heat flow q entering from the atmosphere with a density ρ to a launch vehicle varies to the third power of its speed V [2]:

$$\rho V^3 \sim q \le q_{max}$$

So

$$\frac{d\rho}{\rho} + 3\frac{dV}{V} \le 0$$

and inserting

$$\rho = \rho_0 \exp(-\beta h)$$

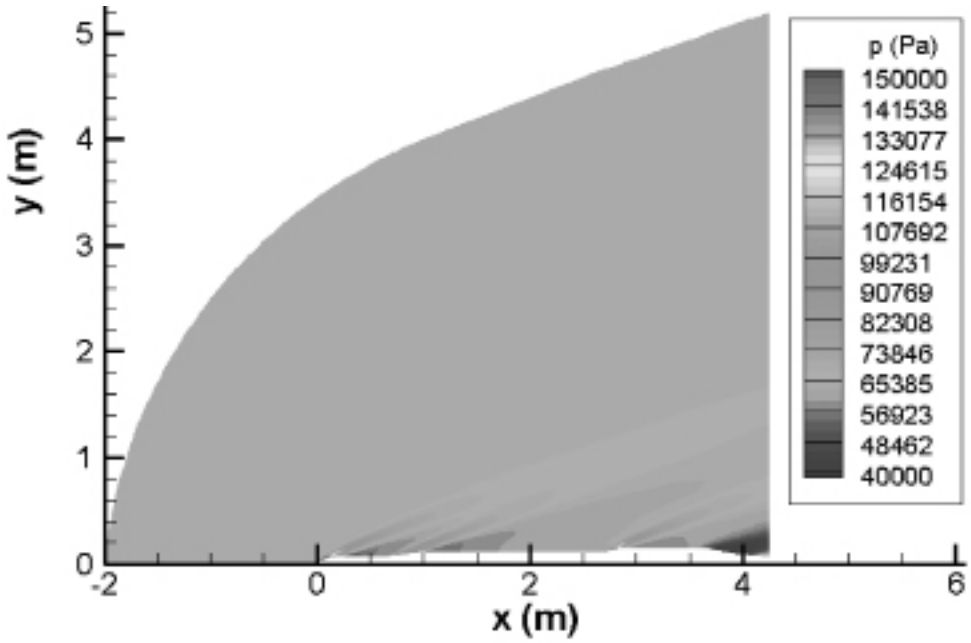


Fig. 3 The static pressure of the atmospheric flow around the rocket at 10 s after launch: flight altitude 3.7 km, Mach 3.1, angle of attack 0 deg.

followed by integration gives a constraint on flight altitude h depending on V:

$$h \geq \frac{3}{\beta} lnV + C \qquad (1)$$

where constant C depends on the thermal limitation for the structure and can be found with the insertion of proper h and V from the trajectory calculated at the first phase of the investigation.

Now considering two kinds of the rocket shell: one made of polypropylene and another made of polypropylene covered with a layer of polytetrafluoroethylene which is sufficient to prevent the shell against melting and reasonably thin to be easily gasified in the rocket engine. Using proper pairs h and V from Fig. 1 for the instants which correspond to Fig. 2(a) and Fig. 2(b), we obtain C = -170900 m for the uncovered shell and C = -186700 m for the covered one if $\beta = 0.000109$ and r_0 = 1.225 kg/m^3. Figure 4 shows two heat border lines corresponding to both the shells according to (1) plotted on the $V - h$ coordinate plane. Figure 4 also illustrates the flights of the CLV initial version (presented in [1] and enhanced with fairings for the obturators) and a modified CILV version designed to meet constraint (1).

One can see that the high level of g-loading of the first stage of the initial CILV trajectory leads to a serious violation of the heat borders, thereby penetrating into the banned area of high heat loads (line 8 in Fig. 4). At the same time high g-loads are necessary to ensure a proper pressure in the rocket gasification chamber; so it is scarcely possible to avoid crossing the heat border by means of decreasing the g-loads. A solution to the problem is a break of the first stage thrust which follows a short initial kick phase (line 1) and continues for some time (line 2) until the passively ascending rocket reaches a high enough altitude with a low density of air, acceptable for the continuation of the flight with a high speed (lines 3 and 4). Figure 4 shows the break corresponding to the moment of reaching the heat border for polytetrafluoroethylene. It is obvious that a thermal protective cover is needed over the polyethylene or polypropylene airframe structure, in order to push the heat boundary to much higher achievable velocities.

However, inserting a pause into the first stage flight causes the problem of the engine burnout and restart. It is possible to propose several ways to resolve this problem. One of them is the insertion of a layer of slowly burning propellant into the main propellant charge (Fig. 5) to keep the gasification chamber hot and slowly move the engine along the rocket while the insertion burns and at the same time having very low thrust. Then as the insertion is burnt the hot engine begins to gasify the main propellant again; and the full thrust flight of the first stage continues until a maximum acceptable g-load is reached in point A (Figs. 4 and 6). At that point the external propellant cylinder is consumed (as described in [1]) and the rocket thrust shifts to a restricted level to reduce g-load. The first stage operates in the restricted mode until the heat and g-load borders are reached again (Figs. 4 and 6); then the first stage structure is separated and the second stage of a traditional low g-load design (presented in [1]) continues the injection of the payload into an orbit.

Figure 5 illustrates the conversion of the rocket configuration while it flies. Figure 6 presents the change of the rocket g-load. Layouts (a), (b), (c) and (d) in Fig. 5 correspond respectively to lines 1, 2, 3 and 4 in Figs. 4 and 6.

In summary the flight trajectory and aerodynamic calculations have verified the theoretical possibility to launch a satellite with the CILV and the estimations of its main parameters made in [1]: the atmospheric losses of speed of about 0.4 km/s (as for traditional LVs) and payload-to-initial mass ratio about 0.005 have been obtained. This mass ratio represents a 1.5 kg payload to orbit for a launcher with an initial mass of 300 kg (while 1 kg was expected according [1]). At the same time the necessity to modify the CILV structure by means of covering its shell with a thermal protection layer and inserting low burning rate propellant in the main charge have been identified.

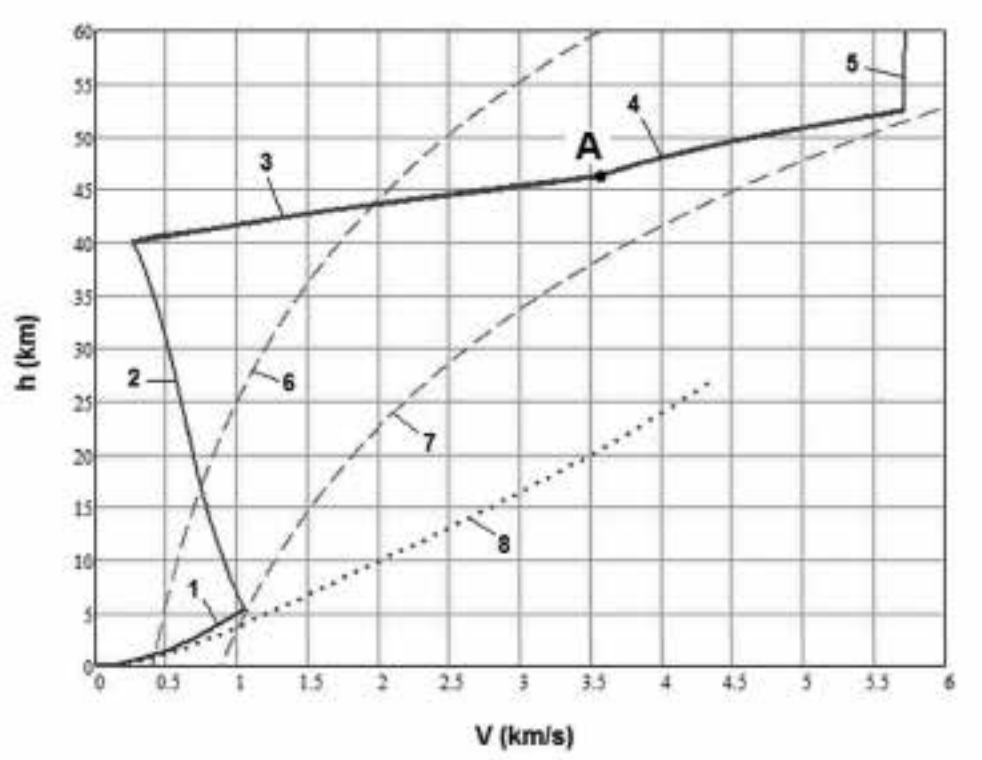


Fig. 4 The phases of the CILV flight and associated heat borders. Key: 1. the first stage of the modified CILV before its passive flight; 2. the passive flight of the modified CILV; 3. the first stage of the modified CILV after its passive flight, full thrust; 4. the first stage of the modified CILV, restricted thrust; 5. the second stage of the modified CILV; 6. the heat border for the polypropylene shell; 7. the heat border for the polypropylene shell covered with polytetrafluoroethylene layer; 8. the first stage of the CILV initial version.

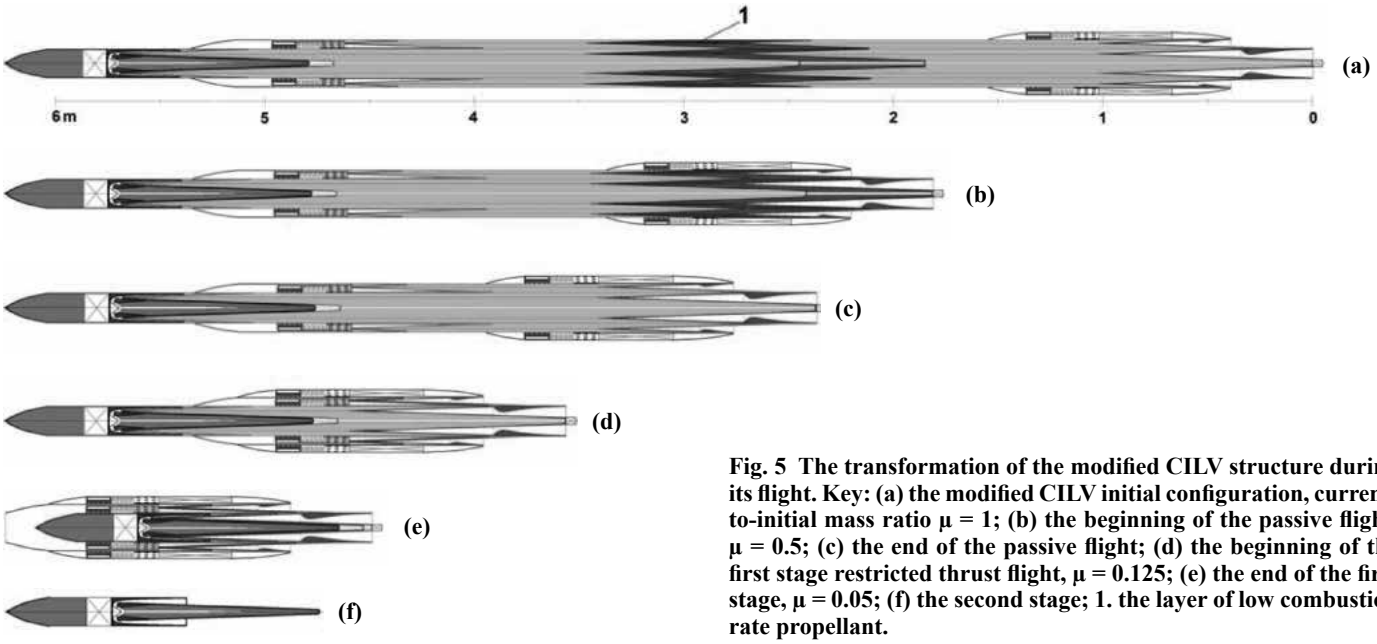


Fig. 5 The transformation of the modified CILV structure during its flight. Key: (a) the modified CILV initial configuration, current-to-initial mass ratio μ = 1; (b) the beginning of the passive flight, μ = 0.5; (c) the end of the passive flight; (d) the beginning of the first stage restricted thrust flight, μ = 0.125; (e) the end of the first stage, μ = 0.05; (f) the second stage; 1. the layer of low combustion rate propellant.

In contrast to a traditional LV the atmospheric flight programme is critical for the CILV. While the atmospheric losses of speed for the traditional LV vary in the limited range from 0.3 to 0.4 km/s the losses for CILVs can be the same or by an order of magnitude greater depending on the atmospheric flight programme. So the programme becomes one of the main design factors – it can make the launching into an orbit possible or not.

As about three metres of the rocket propellant charge, including the slowly burnt insertion, is consumed to get to a height with low enough atmospheric density for full thrust to resume, one obvious launch approach to study would be to launch from an aircraft or from a balloon mounted platform. This will be the topic of further investigation.

3. EXPERIMENTAL INVESTIGATIONS OF THE COAXIAL PROPELLANT CHARGE ENGINE MODEL

3.1 Experimental Plant

Simplicity and low cost must be the main features of a LV. As an engine is the main part of any LV and a gasification chamber (GC) designed to gasify fuel and oxidizer is the main part of the CILV engine [1] then its design is critical. From this point of view the simplest structure of the GC means use of a propellant charge consisting of fuel and oxidizer coaxially layered immediately one next to another without any intermediate matter. Theoretically such a design would be

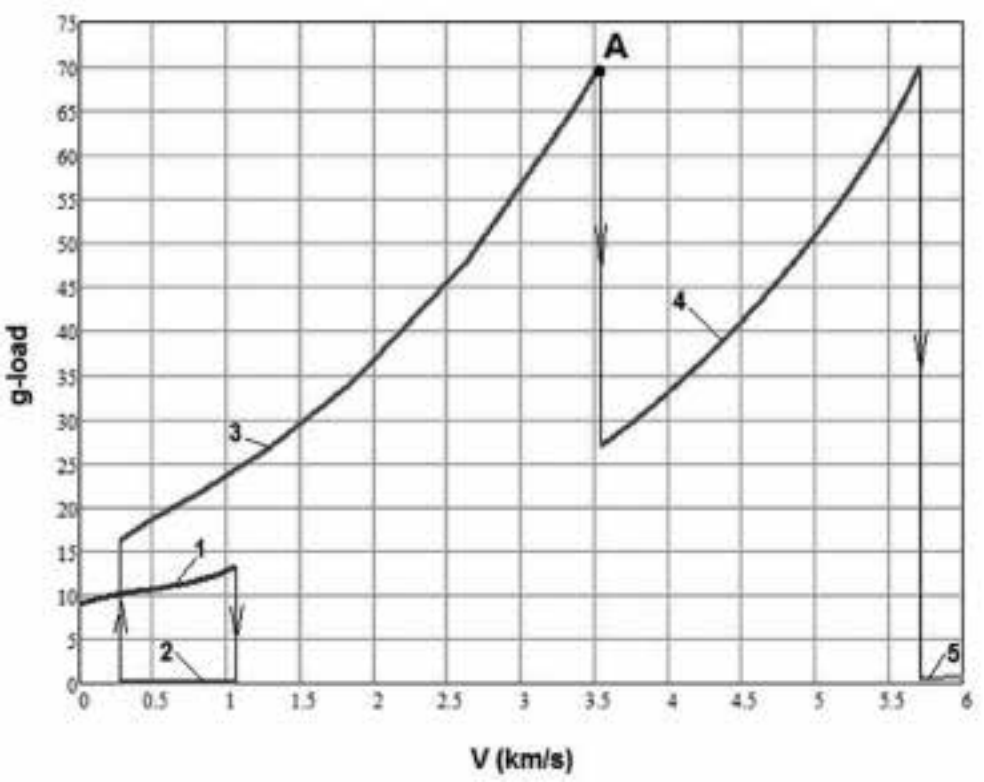


Fig. 6 G-load behaviour during the modified CILV flight. Key: 1. the first stage before its passive flight; 2. the passive flight; 3. the first stage after its passive flight, full thrust; 4. the first stage powered with restricted thrust; 5. the second stage.

dangerous because direct contact of fuel and oxidizer inside the GC near its hot wall can result in spontaneous combustion and a break of the chamber. On the other hand it is possible to suppose that the reacted part of propellant can go out through the nearest injection hole preventing the GC break. To make this detail clear a direct experimental demonstration was required. Figure 7 illustrates the idea of the experiment. The capability to gasify a number of solid fuels and oxidizers, suitable for CLV application, is already well known (Table 1) so the experimental program was aimed at demonstrating the approach chosen for this application.

The main parts of the experimental plant are the GC (18) and the coaxial propellant charge (4) consisting of a polyethylene pipe (10) filled with the solid oxidizer (11) inside. The GC is attached immovable to the thrust rig (1). The propellant charge is fed into the GC by the pneumatic cylinder (2) through the pusher (3) and the guide pipe (6). Hot gases inside the combustion chamber, CC, (19) heat the GC. A contact between the GC and the propellant charge results in gasification of a thin layer of the charge. The gases pass into the CC through injection holes, burn, heat the GC and gasify the next portion of propellant. While the charge is consumed it shortens and the pusher goes into the guide pipe up to the seal (8) (Fig. 7(b)). The seal prevents a breakthrough of gasiform propellant from the GC backwards. To initiate heating the GC, initial propellant is fed into the CC through the injection head (13). After a time initial propellant is cut-off and the main propellant charge gasifies itself. Taps (22) and (23) are used to measure pressure and temperature in the CC.

The GC as the most important part is presented in detail in Fig. 8. The chamber has a single wall perforated with injection holes for passing gasiform propellant outside. The inner surface of the chamber has grooves to collect gases all over the chamber and let them pass to the injection holes. The advantage of such a single-shell structure is its simplicity while its shortcoming is poor

TABLE 1: *Temperatures of Gasification for Several Matters Applicable as Fuels or Oxidizers for CILVs (Degrees Celsius) [3, 4].*

Polyethylene	360…475
Polypropylene	380...450
Polystyrene	350...420
Polyoxymethylene	250...400
Potassium Nitrate	335
Potassium Perchlorate	580
Ammonium Nitrate	200...270
Ammonium Perchlorate	150...300

heating. Propellant components mix and burn mainly beyond the shell in a zone between the GC tip and the CC exhaust opening. To move the combustion zone nearer to the middle of the GC, the injection holes were not drilled in its nose part.

3.2 Test Cell

Combustion testing of the experimental plant was carried out in a rocket motor test cell at the University of Hertfordshire, School of Engineering and Technology. The test cell has a height of about 3.5 m, width of 2.5 m and length of 3 m. It is constructed of multilayer soundproof metal walls, roof and door. The nominal capacity of the cell is for motors up to ½ tonne thrust. The test cell is equipped with gas lines and valves, electric control and data lines. There is an extraction system at a rate of about 1.8 cubic metres per second and two HD cameras to monitor and record firings (Fig. 9).Gaseous propane was used as initial fuel for the experiment. A mixture of gaseous oxygen and nitrogen with a mass ratio ranging from 1:1 to 3:2 or, at the very beginning – nitrous oxide, were used as the

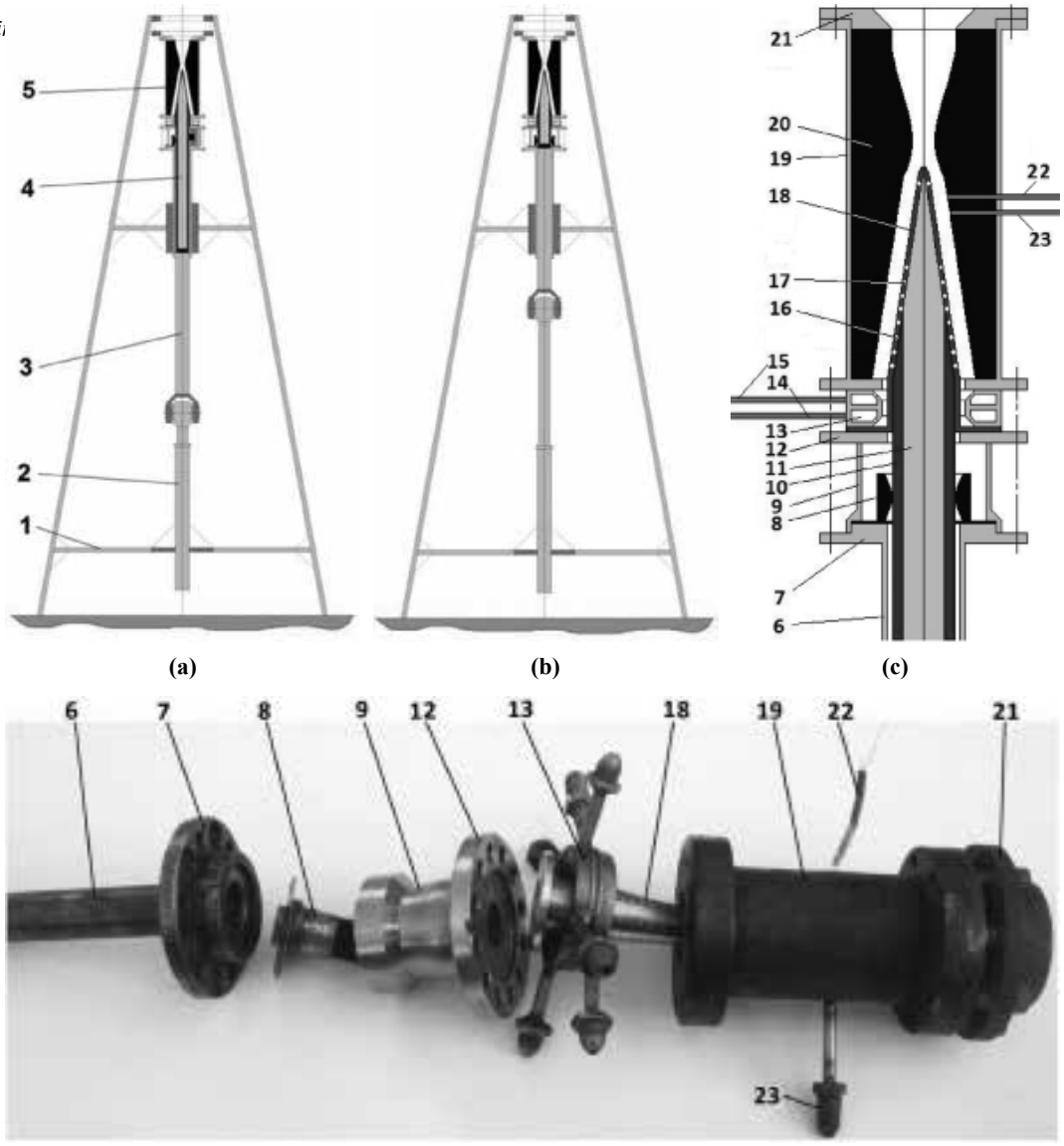


Fig. 7 The present-day configuration of the experimental plant and its main parts. Key: (a) start position; (b) final position: a propellant charge has been fed into an engine by means of a pneumatic cylinder where 1. is the thrust structure; 2. the pneumatic cylinder; 3. the pusher; 4. the propellant charge and 5. the engine; a magnified view of the engine are presented in (c) with the parts photographed in (d) where 6. is the guide pipe; 7. the seal flange; 8. the bearing sleeve seal; 9. the barrel; 10. the tube of polymeric fuel; 11. the core of solid oxidizer; 12. the injection head flange; 13. the injection head; 14. the initial fuel pipe; 15. the initial oxidizer pipe; 16. the fuel holes; 17. the oxidizer holes; 18. the single-shell gasification chamber; 19. the combustion chamber case; 20. the graphite insert; 21. the nozzle flange; 22. a thermocouple and 23. a pressure sensor pipe.

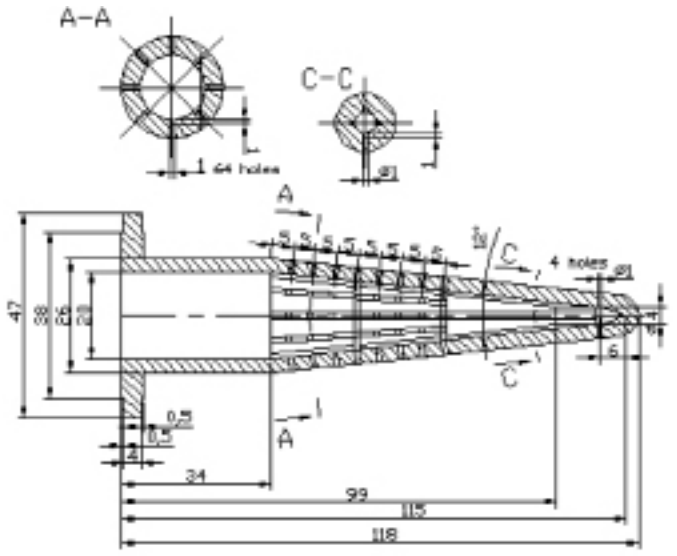
oxidizer. Carbon Dioxide gas drove the pneumatic cylinder. Gas cylinders filled with oxygen and nitrogen were placed outside the test cell. The other gas cylinders were placed inside. An electric arc generated by a high-voltage coil ignited the initial propellant.

Feed pressures were set by means of the adjustable pressure regulators just before tests. Solenoid valves of the gas lines were actuated by means of relays operated with a control panel. The panel, a data logger and video monitor showing firings were placed at a work station at a distance of about 10 metres from the test cell.

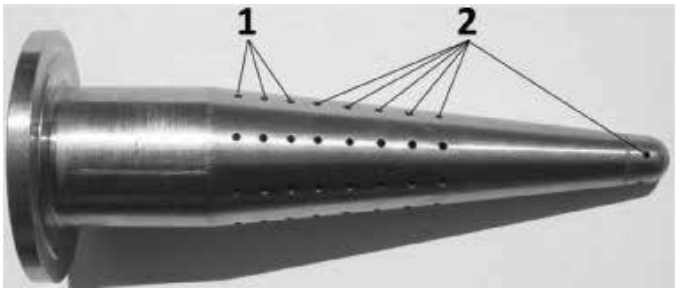
3.3 Course of the Experiment

There were three main stages of the experiment according to three kinds of propellant charge: (1) polyethylene, (2) polyethylene + potassium nitrate and (3) polyethylene + ammonium perchlorate.

At first stage a rod consisted of a polyethylene pipe filled with a polyethylene core was gasified using heat of initial propellant. This was a replication of the earlier experiment made at Dnipropetrovs'k National University [5] to check workability of the equipment. The rod with a length of about 70 mm and diameter of 20 mm was gasified in 21 seconds. Thus its shortening rate was 3 mm per second. Propane and oxygen-nitrogen mixture was used as the initial propellant. Note that at the beginning several attempts were made to use nitrous oxide as the initial oxidizer. This resulted in a cold GC with a temperature less than 100 degrees Celsius. Small pellets of polyethylene remained solid on the outer surface



(a)



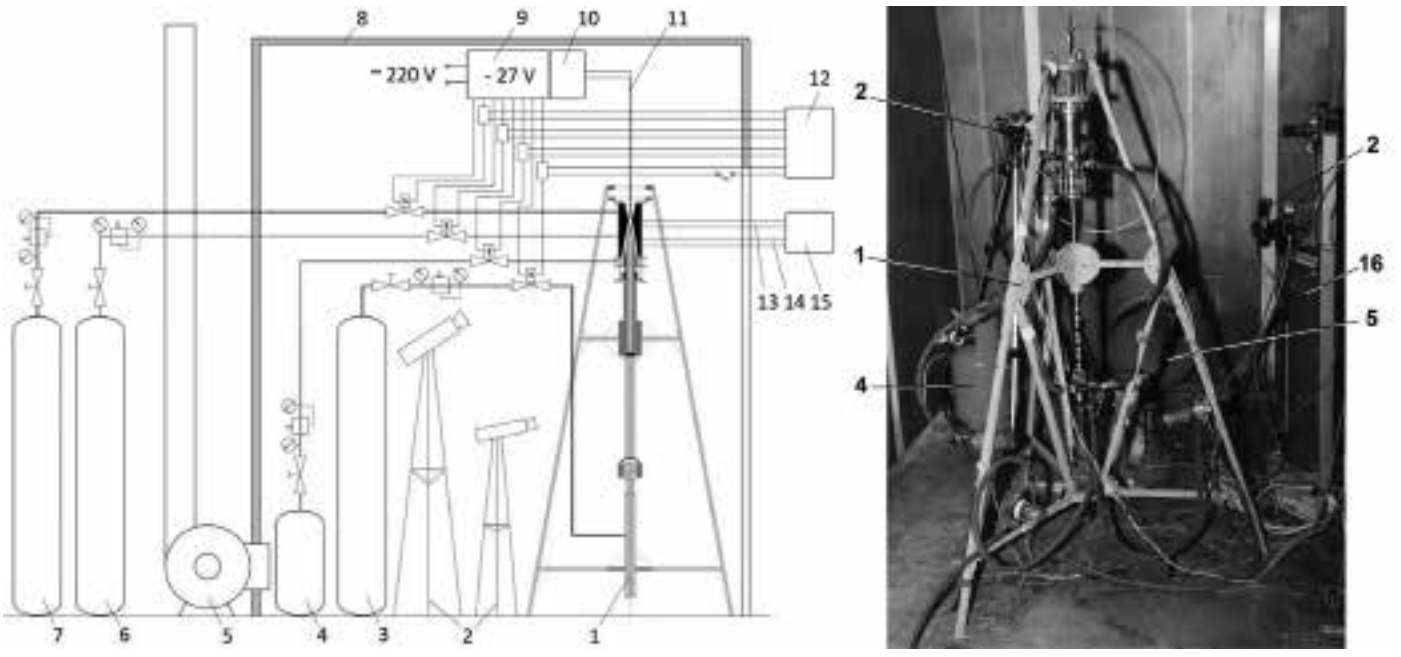
(b)

Fig. 8 The gasification chamber. Key: (a) drawing dimensioned in millimetres; (b) overview; 1. fuel holes; 2. oxidizer holes.

of the GC although the calculated temperature for that initial propellant equalled 2200…2500 K. Discussing the problem, it was supposed that there was insufficient time to break down the nitrous oxide complex compound in the CC because of its rather small volume. Combustion took place out of the CC in the nozzle and outside the nozzle outlet. The nitrous oxide was then changed for oxygen-nitrogen mixture and this then achieved proper heating of the GC.

A second stage polyethylene pipe with a length of about 15 cm and diameter of 2 cm filled with potassium nitrate was gasified and burnt down in 194 seconds. However, before getting such a successful result one more problem was encountered which delayed the experiments for two weeks. There was no motion of the propellant charge despite the action of the pneumatic cylinder force, which could lead to overheating and burning through of the GC. This seemed surprising especially taking into account proven workability of the unit previously. After a series of failures and two lost GCs the cause was found: the propellant rods were made of some more rigid form of polyethylene than used in the first experimental stage. The seal held the rigid rod immobilized, although the same seal let a softer rod pass through. Increasing the seal hole size a little resolved the problem.

The third stage experiments involved the oxidizer being changed for ammonium perchlorate and in this case the charge was gasified and burnt successfully. Figure 10(a) shows the transparent flame of initial propellant heating the GC. After 10 seconds of the initial heating the pusher made a move upwards. After 20 seconds the propellant charge started to burn. This made the exhaust flame brighter and faster (Fig. 10(b)). Flames and the positions of the pusher were monitored with video cameras. The feed of initial fuel was cut off just as the visible part of the pusher shortened up to 5 cm. From this instant self-sustain combustion



(a) **(b)**

Fig. 9 The experimental rig in the rocket motor test cell. Key: (a) layout of the main equipment; (b) overview showing 1. the experimental rig; 2. the video camera; 3. the carbon dioxide cylinder; 4. the propane bottle; 5. the extractor of combustion products; 6. the oxygen cylinder; 7. the nitrogen cylinder; 8. the walls, roof and door; 9. the electric power supply; 10. the high voltage coil; 11. the high voltage wires; 12. the control panel; 13. the temperature sensor line; 14. the pressure sensor line; 15. the data logger and 16. the nitrous oxide bottle.

of the propellant charge was observed (Fig. 10(c)). The process was rather slow and accompanied by decreasing of the shortening rate and CC pressure because the flow of combustion products did not pass over the GC and could not heat it effectively. As seen in Fig. 10(d and e) the stroke of the pneumatic cylinder was 20 cm – every mark on the pusher being 5 cm. A part of the propellant rod, with a length of 15 cm, was therefore gasified and burnt by means of initial propellant (for 74 seconds) and the rest was consumed in self-sustain mode.

There was one successful test in the third phase. Another one failed. The success ensued from proper initial charging of the GC (Fig. 11(a)) while wrong filling of the GC (Fig. 11(b)) caused detonation of oxidizer and destruction of the rig (Fig. 11(c)) as soon as the initial flame touched the holes of the GC filled with oxidizer.

Despite the problems and the explosion, the workability of a GC designed for a coaxial charge of fuel and oxidizer, which are separated without any intermediate layer, was demonstrated for the first time.

Table 2 presents the feed pressure settings and the shortening rates determined at complex mode of heating by means of initial and main propellants.

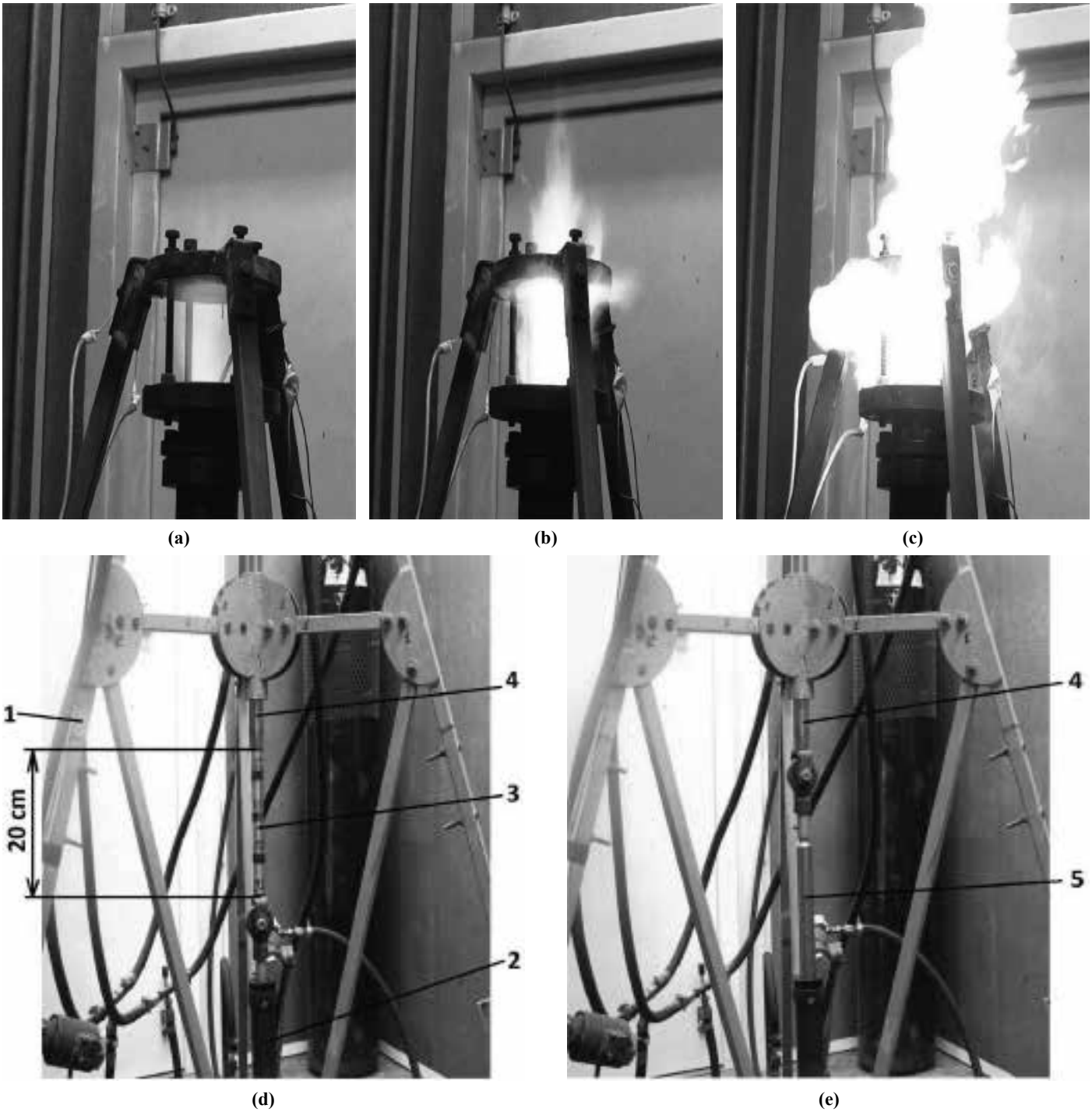
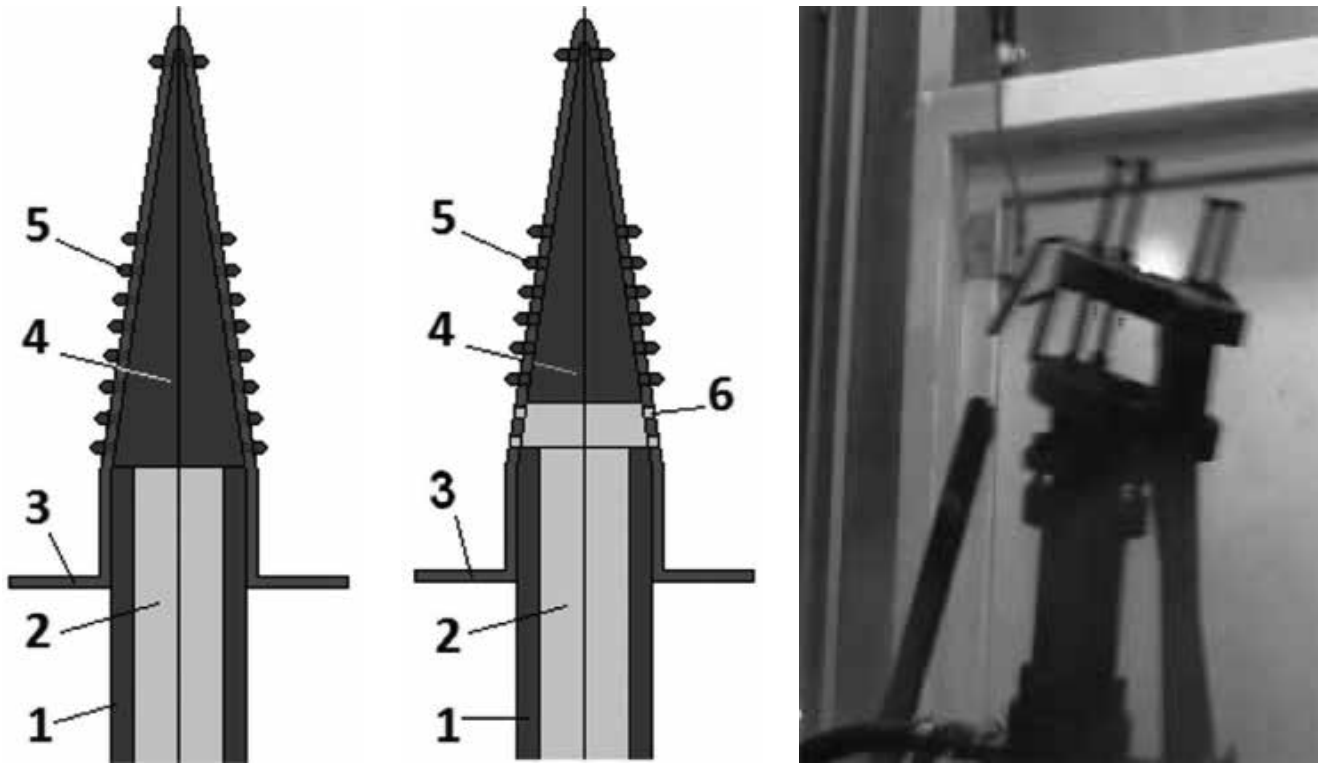


Fig. 10 The course of a third phase test. Key: (a) heating the gasification chamber by means of initial propellant, propane + oxygen + nitrogen; (b) burning main propellant, polyethylene + ammonium perchlorate, together with initial propellant; (c) self-sustaining burning of the main propellant without initial propellant; (d) initial position of the pusher; (e) final position of the pusher where 1. is the experimental structure; 2. the pneumatic cylinder; 3. the pusher; 4. the guide pipe and 5. the rod of the pneumatic cylinder.



(a) (b) (c)

Fig. 11 Initial charging of the gasification chamber. Key: (a) successful; (b) unsuccessful resulting in (c) the damaged rig where 1. is the polymeric fuel pipe; 2. the solid oxidizer; 3 the gasification chamber; 4. the polymeric fuel insert; 5. the pellets formed by excessive fuel going through the injection holes and 6. the holes filled with oxidizer.

TABLE 2: *Setting the Gas Supply and the Achieved Shortening Rates of Propellant Charge.*

Propellant Charge	Feed Pressure (MPa)/Flow Rate (kg/s)				Shortening Rate (m/s)
	Propane	Oxygen	Nitrogen	CO2	
Polyethylene	0.4/0.0017	0.7/0.0030	1.0/0.0030	1.5/-	$3.0 \cdot 10^{-3}$
Polyethylene + Potassium Nitrate	0.3/0.0015	0.5/0.0026	0.5/0.0017	1.5/-	$0.8 \cdot 10^{-3}$
Polyethylene + Ammonium Perchlorate	0.3/0.0015	0.5/0.0026	0.5/0.0017	1.5/-	$2.0 \cdot 10^{-3}$

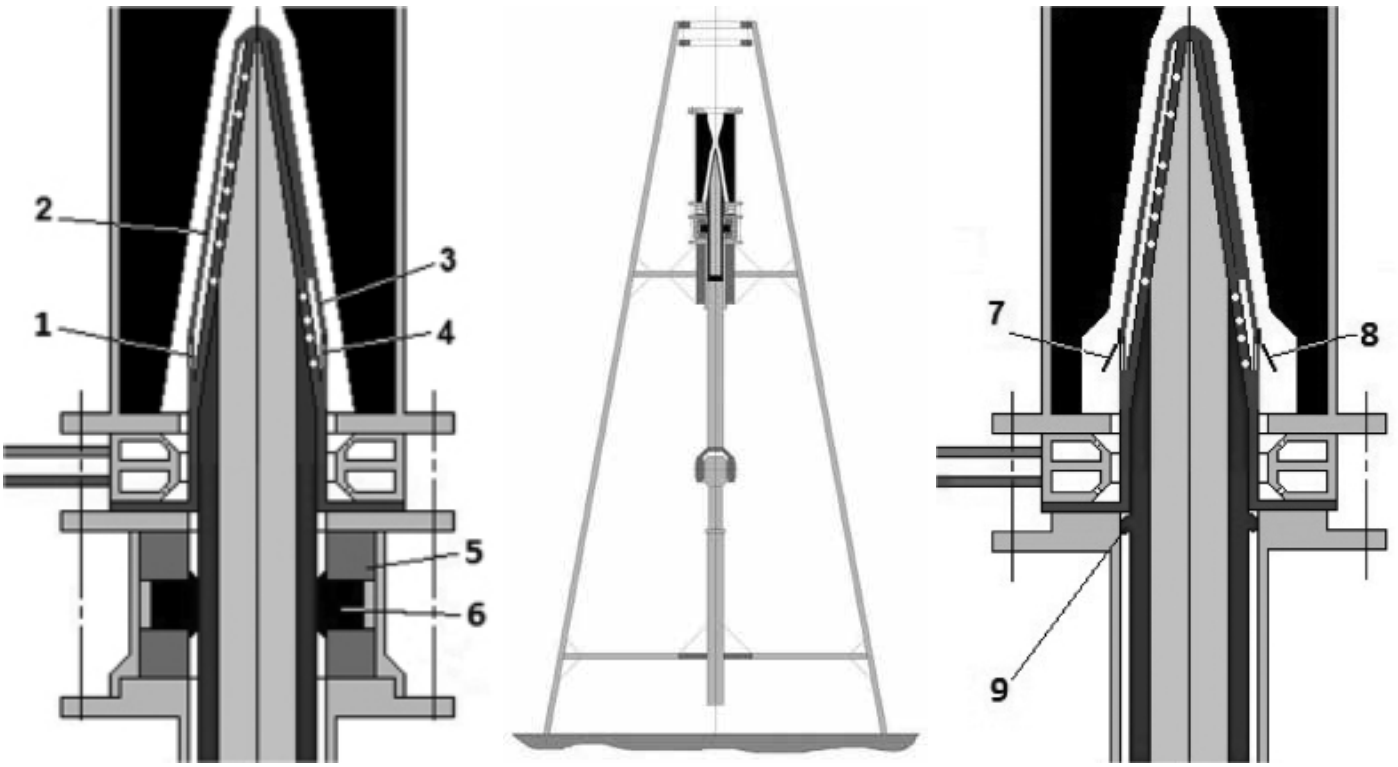
3.4 The Next Tests

As it is pointed out in [1] a CILV can be realized if the shortening rate of its case is 10^{-1} metres per second. This is two orders of magnitude larger than the figures obtained here, and presented in Table 2. The task of the next work is therefore increasing the shortening rate attainable with the experimental plant. We plan to pay particular attention on modifications of the GC design.

The well-known minimal burn rate of solid propellant – or its gasification rate, which is the same in this case – equals 10^{-3} metres per second. Taking into account that the 6 degree cone half angle GC presented in Fig. 8 has to ensure a shortening rate 10 times greater than a gasification rate, we should obtain 10^{-2} metres per second shortening rate in the tests presented, instead of 10^{-3} metres per second. It is suggested that such a low shortening rate results from several causes such as weak heating, too tight seal and too small injection holes. It is therefore proposed to increase the shortening rate during the next tests by making several modifications. The idea is the redirection of gasiform oxidizer and fuel streams from the tip to the root of the GC by means of longitudinal ducts inside its double-shell wall (Fig. 12(a)). For a propellant rod with a diameter of $2 \cdot 10^{-2}$ metres and a cross section of about $3 \cdot 10^{-4}$ square metres the increase of the shortening rate up to 0.03-0.05 metres per second corresponds to a 30-50 gram per second of propellant consumption, a 60-100 N thrust and a 0.2-0.3 MPa gauge pressure in the GC if the specific impulse of the engine and the propellant density are to be about 2000 metres per second and 3000 kg per cubic metre respectively.

It is also expected that more shortening rate, thrust and GC pressure will be achieved by means of decreasing the GC angle by up to 3 degree. This, theoretically, can give up to 0.1 metres per second, 200 N and 0.6 MPa respectively. This is just near the threshold of the inertial self-feeding rocket engine feasibility. Such an engine would be capable of moving itself along the propellant rod by means of its own thrust if the pneumatic pusher is cut off (Fig. 12(b)).

Another way to get self-feeding is use of a pulsed mode of engine operation. It is known that a pulsed engine operates even if its combustion chamber pressure is much more than its feed pressure. For the present case this means that the CC pressure can be bigger than the GC pressure. The GC equipped with valves as shown in Fig. 12(c) can theoretically operate at the shortening rate with an order of 10^{-2} metres per second and GC pressure with an order of 10^{-1} MPa. These figures are more easily achieved than necessary ones for the inertial



(a) (b) (c)

Fig. 12 The future configuration of the experimental rig (start position is presented in Fig. 7(a)). Key: (a) a double-shell gasification chamber engine; (b) final position when the engine has consumed the propellant charge by means of its own thrust; (c) a pulsed engine option where 1. is the oxidizer injector; 2. the oxidizer duct; 3. the fuel duct; 4. the fuel injector; 5. a permanent magnet; 6. ferropowder; 7. the oxidizer valve; 8. the fuel valve and 9. the collar of melted polymeric fuel.

mode. A pulsed self-feeding engine therefore has a chance to be developed before an inertial one if the problems of its valve design and operation are resolved.

Several minor modifications will also be made to the GC seal. A collar of melted polyethylene will be used as a kind of seal for a low-pressure GC (Fig. 12 (c)). A ferropowder seal [1] will be applied for a GC of bigger pressure (Fig. 12 (a)).

4. CONCLUSIONS

1. The flight programme of the CILV must include a pause during its atmospheric phase; the rocket case needs some thermal protection.
2. A coaxial propellant charge can be used without intermediate layers between fuel and oxidizer as a case for the CILV.
3. Modifications of the GC structure are necessary to get the high shortening rate and make the CILV feasible.
4. A pulsed mode of the CILV engine theoretically allows the decreased required shortening rate and GC pressure. The lesser required GC pressure gives a possibility to shorten the minimal acceptable length of a CILV propellant charge from 6 metres according to [1] up to 1-2 metres. A conceptual design of such a pulse CILV is illustrated in Fig. 13. The flight profile of such a pulse rocket, and the comparison of it with the inertial rocket of the same initial-to-payload mass ratios are presented in Fig. 14. This approach can pioneer a new technology of small and short LVs for pico (10^{-1} kg) and femto (10^{-2} kg) satellites combined with advantages of MEMS technology. Additional shortening of the LVs is theoretically possible by means of greater initial acceleration combined with an increase of the rocket forward diameter to increase the corresponding

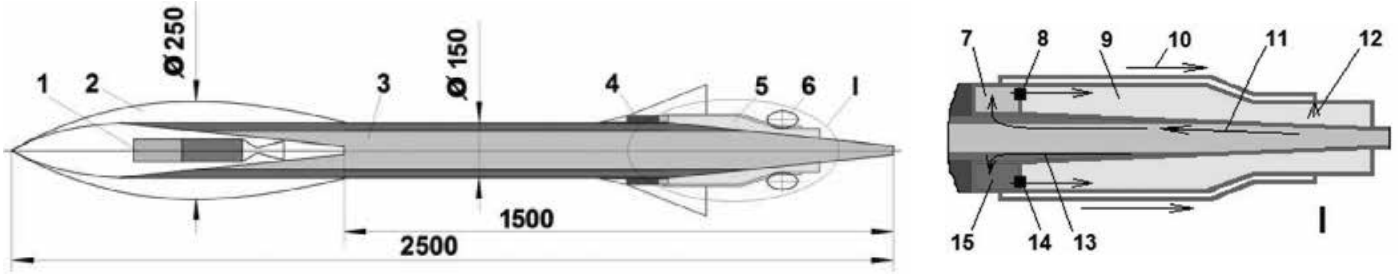


Fig. 13 A small combustible pulse LV concept with an initial mass of about 50 kg capable of orbiting a 100 g payload into a low orbit. Dimensions are in millimetres. Key: 1. the payload attached 2nd solid stage; 2. a variable geometry inflatable nose fairing; 3. the combustible case of polymeric pipe filled with solid oxidizer; 4. an obturator; 5. the mobile engine; 6. a restart system; 7. the oxidizer chamber; 8. the oxidizer valve; 9. the combustion chamber; 10. gasiform propellant component flow to control injector; 11. gasiform oxidizer flow; 12. a control injector; 13. gasiform fuel flow; 14. the fuel valve and 15. the fuel chamber.

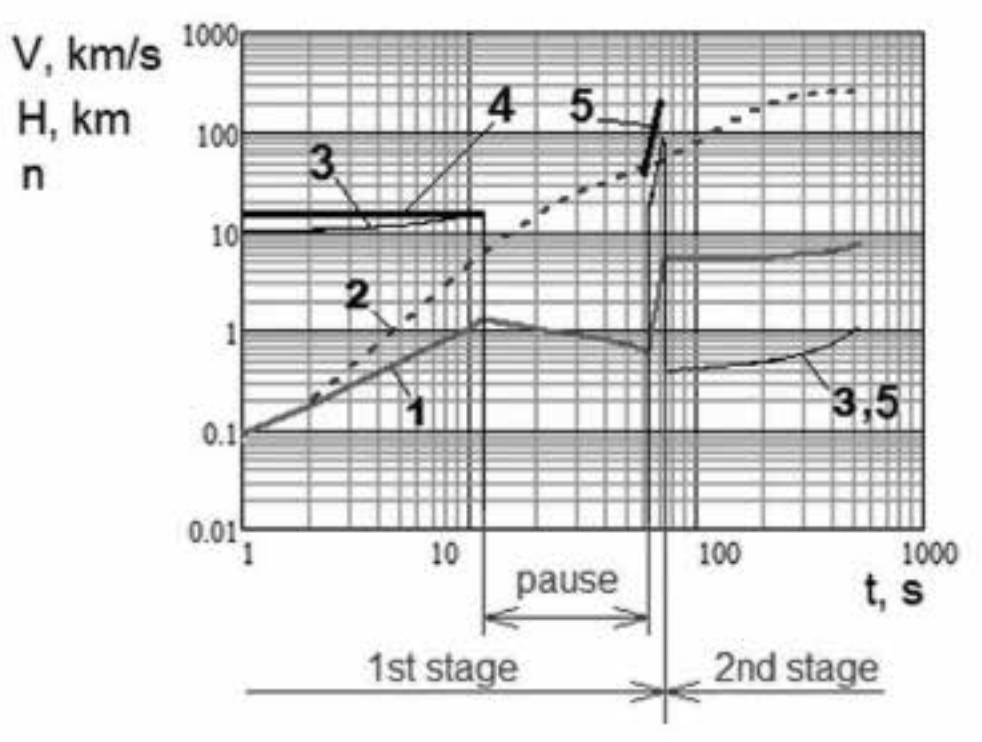


Fig. 14 Combustible inertial and pulse small LVs flight speed V, altitude H and g-load n versus time. Key: 1. V for both the LVs; 2. H for both the LVs; 3. n for the inertial LV; 4. n for the pulse LV with the inflated fairing and 5. n for the pulse LV with the blown off fairing.

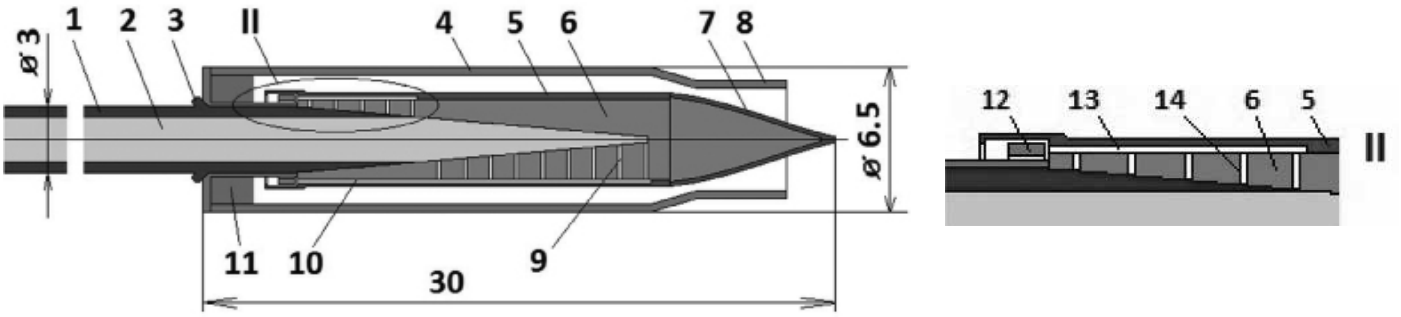


Fig. 15 Propellant cartridge of a self-feeding micropropulsion unit. Dimensions are in millimetres. Key: 1. polymeric fuel; 2. solid oxidizer; 3. seal – a collar of melted fuel; 4. the combustion chamber case; 5. the gasification chamber steel case; 6. the gasification chamber of copper; 7. thermal coating; 8. the nozzle; 9. an oxidizer hole; 10. the oxidizer duct; 11. the space for a solid propellant igniter; 12. the ring valve; 13. the fuel duct and 14. a fuel hole.

aerodynamic drag to limit the LV speed at low heights to prevent excessive frictional thermal loads. This can be realized in practice by means of an active variable geometry nose fairing (possibly an inflatable design).

Moreover, a pulse self-feeding propulsion unit with a structure of simple design could be miniaturized and applied for small spacecraft propulsion. The advantage of such a unit would be the absence of propellant tanks and feed systems. A conceptual design of such a micropropulsion unit with a thrust of 0.1-0.2 N is proposed in Fig. 15. A satellite can be equipped with a magazine and dispenser of such cartridges to provide a range of impulse options in different directions.

REFERENCES

1. V. Yemets, F. Sanin, O. Kostritsyn, M. Masliany and G. Minteev, "Is the Combustible Inertial Pico Launch Vehicle Feasible?", *JBIS*, **63**, pp.249-259, 2010.
2. V.P. Mishin, V.K. Bezverby, B.M. Pankratov and D.N. Shcheverov, "*The Design Basis of Flight Vehicles (Transport Systems)*", Mashinostroenie Publishing House, Moscow, 1985 (in Russian).
3. A. Schwarz and G. Cramer, "Chemical Stability and Physical-Chemical Properties of Polythene", in *Polythene*, ed. A. Renfrew and Ph. Morgan, London – New York, p.231, 1960.
4. I.L. Knunyants (chief ed), "Chemical Encyclopaedia", **Vol. 1, 2, 3**, Soviet Encyclopaedia Publishing House – Big Russian Encyclopaedia Publishing House, Moscow, 1988-1992 (in Russian).
5. V. Yemets, F. Sanin, Y. Dzhur, M. Masliany, O. Kostritsyn and G. Minteev, "Single Stage Small Satellite Launcher with Combustible Tank of Polyethylene", *Acta Astronautica*, **64**, pp.28-32, 2009.

(Received 23 September 2014; Accepted 18 November 2015)



https://dspace.org/

Investigations of a combustible inertial launch design

Yemets, V.; Prince, Simon A.; Wilkinson, Ray

2015-06-30
British Interplanetary Society
https://www.jbis.org.uk/paper/2015.68.188
Yemets V, Prince SA, Wilkinson R. (2015) Investigations of a combustible inertial launch design. Journal of the British Interplanetary Society, Volume 68, Issue 7, pp. 188-199

Downloaded from a DSpace repository. https://dspace.org/